Paper presented at the IEEE International Ultrasonics Symposium, Prague, Czech Republic, 2013:

Non-invasive Measurement of Pressure Gradients in Pulsatile Flow using Ultrasound

Jacob Bjerring Olesen[1], *Marie Sand Traberg*[1], *Michael Johannes Pihl*[1],
Peter Møller Hansen[2], *Michael Bachmann Nielsen*[2] *and*
Jørgen Arendt Jensen[1]

[1]Center for Fast Ultrasound Imaging,
Biomedical Engineering group, Department of Electrical Engineering, Bldg. 349,
Technical University of Denmark, DK-2800 Kgs. Lyngby, Denmark

[2]Department of Radiology, Copenhagen University Hospital, Rigshospitalet, Denmark

To be published in Proceedings of IEEE International Ultrasonics Symposium, Prague, Czech Republic, 2013.

Non-invasive Measurement of Pressure Gradients in Pulsatile Flow using Ultrasound

Jacob Bjerring Olesen*, Marie Sand Traberg*, Michael Johannes Pihl*, Peter Møller Hansen†, Michael Bachmann Nielsen† and and Jørgen Arendt Jensen*

*Center for Fast Ultrasound Imaging, Dept. of Elec. Eng., Bldg. 349,
Technical University of Denmark, DK-2800 Kgs. Lyngby, Denmark
†Department of Radiology, Rigshospitalet, DK-2100 Copenhagen, Denmark

***Abstract*—This paper demonstrates how pressure gradients in a pulsatile flow environment can be measured non-invasively using ultrasound. The proposed method relies on vector velocity fields acquired from ultrasound data. 2-D flow data are acquired at 18-23 frames/sec using the Transverse Oscillation approach. Pressure gradients are calculated from the measured velocity fields using the Navier-Stokes equation. Velocity fields are measured during constant and pulsating flow on a carotid bifurcation phantom and on a common carotid artery *in-vivo*. Scanning is performed with a 5 MHz BK8670 linear transducer using a BK Medical 2202 UltraView Pro Focus scanner. The calculated pressure gradients are validated through a finite element simulation of the constant flow model. The geometry of the flow simulation model is reproduced using MRI data, thereby providing identical flow domains in measurement and simulation. The proposed method managed to estimate pressure gradients that varied from 0 kPa/m–7 kPa/m during constant flow and from 0 kPa/m–200 kPa/m in the pulsatile flow environments. The estimator showed, in comparison to the simulation model, a bias of -9% and -8% given in reference to the peak gradient for the axial and lateral gradient component, respectively.**

I. Introduction

Local pressure gradients in hemodynamics can provide important information for diagnosing various cardiovascular diseases such as atherosclerosis [1]. The gradients can be used as an indication on how changes in the flow, for instance caused by plaque formation, affect the risk of embolism. Current measures of pressure gradients are acquired using catheters inserted into a larger artery and threaded to the region of interest. Although this procedure is reported reliable and of low risk, it remains an invasive procedure. A less invasive method for measuring the local pressure gradients was proposed by Fairbank and Scully [2]. The method relies on injecting contrast agent microbubbles into the circulatory system and measuring the frequency shift in the scattered spectrum as ultrasonic waves are applied. Despite the less invasive procedure, it still requires the injection of microbubbles. Furthermore, it only provides a short time window for imaging as the bubbles are taken up by the liver or rupture due to the acoustic pressure field produced by the ultrasound transducer. This paper presents pressure gradients estimated from ultrasound vector velocity data by exploiting the Transverse Oscillation (TO) method developed by Jensen and Munk [3] and Anderson [4] who suggested a similar approach. The TO method is able to estimate the two spatial velocity components within the ultrasound scan plane independently of each other. This allows for determination of flow patterns such as vortices or other complex features that are likely to occur when fluid passes through a constricted vessel. The purpose of this paper is to show that pressure gradients can be measured non-invasively using ultrasound with the long-term aim of replacing or assisting catheterization. The paper compares pressure gradients estimated using the Navier-Stokes equation to gradients that is simulated in a finite element model.

II. Methods

The following section presents the method used for calculating pressure gradients from vector velocity data using the Navier-Stokes equation. For an isotropic incompressible Newtonian fluid it is given by

$$\rho\left[\frac{\partial \mathbf{v}}{\partial t} + \mathbf{v}\cdot\nabla\mathbf{v}\right] = -\nabla p + \rho\mathbf{g} + \mu\nabla^2\mathbf{v}. \tag{1}$$

The equation describes the development of fluid velocity $\mathbf{v} = (v_x, v_y, v_z)$ by relating the body forces acting on the isotropic fluid volume to its acceleration and density, where ρ is the density of the fluid and μ its viscosity. The left-hand terms sum the local $\frac{\partial \mathbf{v}}{\partial t}$ and convective acceleration $\mathbf{v}\cdot\nabla\mathbf{v}$ of the velocity, where ∇ is the spatial differential operator $(\frac{\partial}{\partial x}, \frac{\partial}{\partial y}, \frac{\partial}{\partial z})$. The right-hand side sum-up the surface and volume forces, which include the desired pressure gradient $-\nabla p$, as well as a gravitational force $\mathbf{g}$ acting on the fluid volume and a viscous drag caused by the viscosity of the fluid $\mu\nabla^2\mathbf{v}$, where $\nabla^2\mathbf{v}$ is the Laplacian of the velocity. For clinical applications, the effect of the viscous term in (1) can be omitted as this has no significant influence on flow in larger vessels [5], [6]. A patient undergoing an ultrasound scan is usually placed in a horizontal position, so the gravitational term can be neglected as well. The pressure gradient is, thus, directly linked to the acceleration field of the fluid, which is derived from the velocity field $\mathbf{v}$:

$$\nabla p = -\rho\left[\frac{\partial \mathbf{v}}{\partial t} + \mathbf{v}\cdot\nabla\mathbf{v}\right]. \tag{2}$$

Eq. (2) states that all three vector components of $\mathbf{v}$ must be known to estimate the pressure gradient $-\nabla p$. Using the TO approach and a 1-D linear array the two-dimensional in-plane velocity vector can be measured. The proposed method for estimating the pressure gradients is therefore developed assuming that the out-of-plane velocity v_y is zero, (though, the

$$\frac{\Delta \mathbf{P}(i,j,k)}{\Delta x} \simeq \frac{-\rho}{2\Delta t}\Big(\mathbf{V}_x(i,j,k+1) - \mathbf{V}_x(i,j,k-1)\Big) - \rho \begin{bmatrix} \mathbf{V}_x(i,j,k)/2\Delta x \\ \mathbf{V}_z(i,j,k)/2\Delta z \end{bmatrix} \cdot \begin{bmatrix} \mathbf{V}_x(i-1,j,k) - \mathbf{V}_x(i+1,j,k) \\ \mathbf{V}_x(i,j-1,k) - \mathbf{V}_x(i,j+1,k) \end{bmatrix}$$
$$\frac{\Delta \mathbf{P}(i,j,k)}{\Delta z} \simeq \frac{-\rho}{2\Delta t}\Big(\mathbf{V}_z(i,j,k+1) - \mathbf{V}_z(i,j,k-1)\Big) - \rho \begin{bmatrix} \mathbf{V}_x(i,j,k)/2\Delta x \\ \mathbf{V}_z(i,j,k)/2\Delta z \end{bmatrix} \cdot \begin{bmatrix} \mathbf{V}_z(i-1,j,k) - \mathbf{V}_z(i+1,j,k) \\ \mathbf{V}_z(i,j-1,k) - \mathbf{V}_z(i,j+1,k) \end{bmatrix} \quad (3)$$

method can be extended to use full three-dimensional data). The two in-plane vector components of the pressure gradient are calculated using a finite central difference approximation [7]. The equations in (3) show how the vector components are calculated discretely for each position in the scan plane at every frame. $\mathbf{V}_x$, $\mathbf{V}_z$ and $\frac{\Delta \mathbf{P}}{\Delta x}$, $\frac{\Delta \mathbf{P}}{\Delta z}$ denote two-dimensional fields of discrete vector velocity components and pressure gradient components, respectively. The index position within each field is given by (i, j), while *k* represents the field or scan frame being calculated. Each consecutive field is separated in time by $\frac{1}{framerate} = \Delta t$. The Δx and Δz are the sampling interval of the velocity field in the axial and lateral direction, respectively. The calculated pressure gradients in each scan frame are low-pass filtered using a 2-D Hann window $\mathcal{H}_{2D}$ to reduce noise from the numerical differentiation.

III. Experimental Setup

A BK Medical 2202 UltraView Pro Focus scanner (BK Medical, Herlev, Denmark) equipped with an UA2227 research interface is used for obtaining ultrasound RF data. A C70-SSEA flow phantom (Shelley Medical Imaging Technologies, Toronto, Canada) is scanned using a BK8670 linear array transducer at 18 and 21 frames per second, depending on the study. The flow phantom models a carotid artery having a constriction at the beginning of the internal branch, as seen in Fig. 1. The phantom is embedded in agar to mimic the characteristics of human tissue, and it is encased in an air tight acrylic box with an acoustic window making it compatible with ultrasound imaging as well as MRI. For the steady flow set-up, a constant flow rate of 1.0 mL/s is selected, while the pulsatile flow profile is set to mimic a simplified carotid profile with a period of 0.84 seconds and a flow rate of 5.0 mL/s. Blood-mimicking fluid is used with a density of 1,037 kg/m^3 and a viscosity of 4.1 mPa·s.

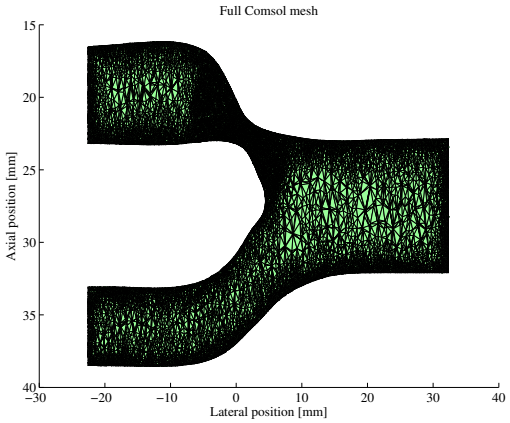

Figure 1. Outline of the flow phantoms fluid domain.

The accuracy of the pressure gradients estimated under steady flow conditions is evaluated through comparison to a finite element model. The geometry of this model is constructed from MRI data of the flow phantom performed at the Department of Diagnostic Radiology at Rigshospitalet, Denmark, using a 3 Tesla Magnetom Trio scanner (Siemens, Munich, Germany). The finite element model was composed of more than 600,000 tetrahedrons, which were especially dense in the constricted region of the phantom to ensure a high spatial resolution. The simulation study was carried out using Comsol (v4.2a, Stockholm, Sweden).

An *in-vivo* study of the common carotid artery on a healthy male volunteer was also made. The study was made using a pulse repetition frequency of 5.1 kHz for capturing 23 frames per second.

IV. Results

The following section presents the results of the proposed estimator. The flow data used for validating the estimator were captured from the carotid flow phantom at the site of the constriction at 18 frames/sec. The result of the *in-vivo* study is shown at the end of the section.

A. Constant flow measurement

A vector velocity map of the flow through the constricted area of the phantom is plotted in Fig. 2 along with the estimated and simulated pressure gradients. The fluid flows from right to left and reaches a peak velocity of 0.15 m/s at the centre of the constriction. The centre panel in Fig. 2 shows the estimated pressure gradients calculated using the velocities in the left panel. The right-hand side of the figure shows the simulated pressure gradients. The background color and length of the arrows indicate the magnitude of the pressure gradients or velocity vectors, respectively. The arrows' direction indicates the angle of the vector. The two gradient plots display arrows that tend to point away from the centre of the constriction, indicating that a low pressure is present here, as a gradient always point in direction of increasing values.

Fig. 3 shows the result of the estimator taken along the red-dotted lines which run parallel to the fluid flow in Fig. 2. The results show a mean magnitude of the axial and lateral pressure gradients along with $\pm$ one standard deviation of the estimates. The blue line shows the simulated pressure gradients along the same path. The estimator produced pressure gradients of magnitudes varying from -3 kPa/m to 10 kPa/m with a bias normalized to the peak gradient of -9% and -8% for the axial and lateral vector component, respectively. The standard deviation when using the mean of two successive velocity frames for each estimate were 28% and 65% for the axial and lateral component.

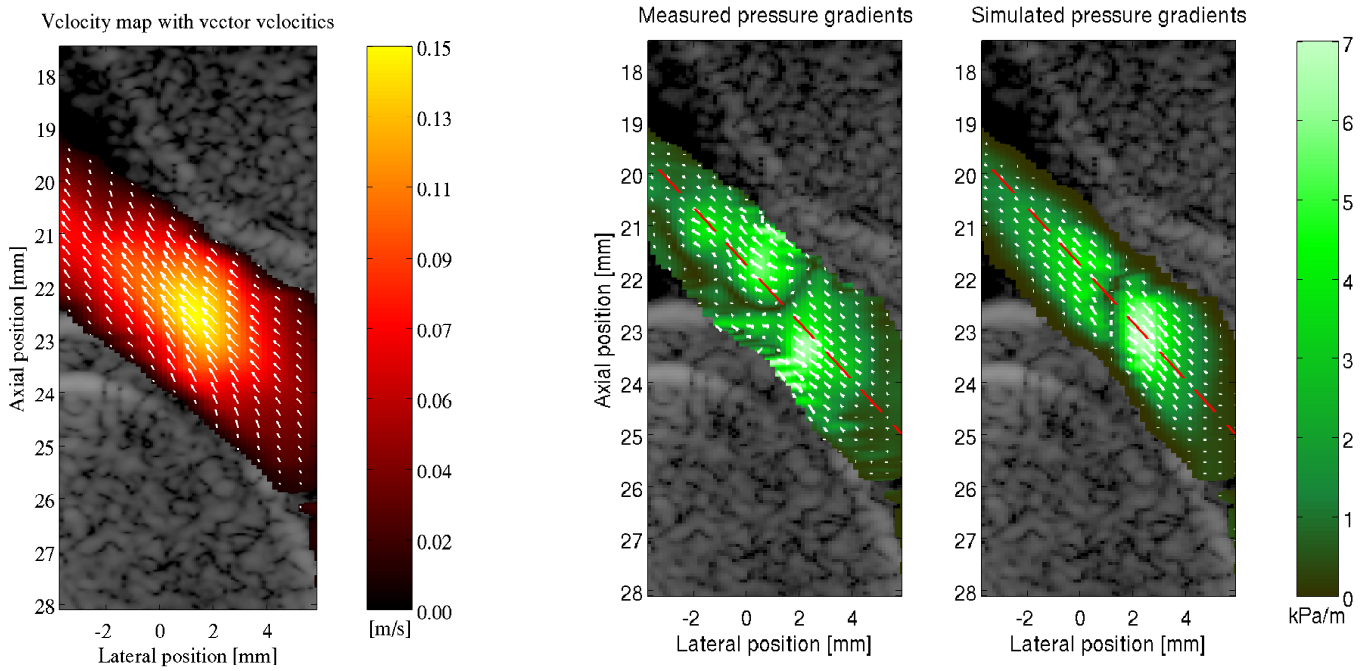

Figure 2. Vector velocity map along with the estimated and simulated pressure gradients. The left panel shows a vector velocity map of the blood mimicking fluid that flows through the constriction from right to left. The centre panel shows the pressure gradients estimated from vector velocity data, while the panel to the right shows the simulated gradients.

B. Pulsating flow measurement

Pressure gradients estimated from velocity data acquired at 21 frames/sec from the flow phantom during pulsatile flow are shown in Fig. 4. The graphs display both the mean velocity and the mean gradients over an area of $0.4\,\mathrm{mm}^2$, which is located just left of the centre of the constriction. The displayed gradients have been low-pass filtered by a normalized Hanning window across the velocity frames corresponding to 9 frames. The size of the gradients varies from 5 kPa/m in diastole to roughly 150 kPa/m in peak systole. The pressure gradients seen in the pulsatile flow measurement are more than twenty times greater at peak systole than the gradients measured during constant flow conditions, despite the flow rate being only five times larger. Thus, indicating that temporal changes in flow velocities play a dominant role in the magnitude of the pressure gradients.

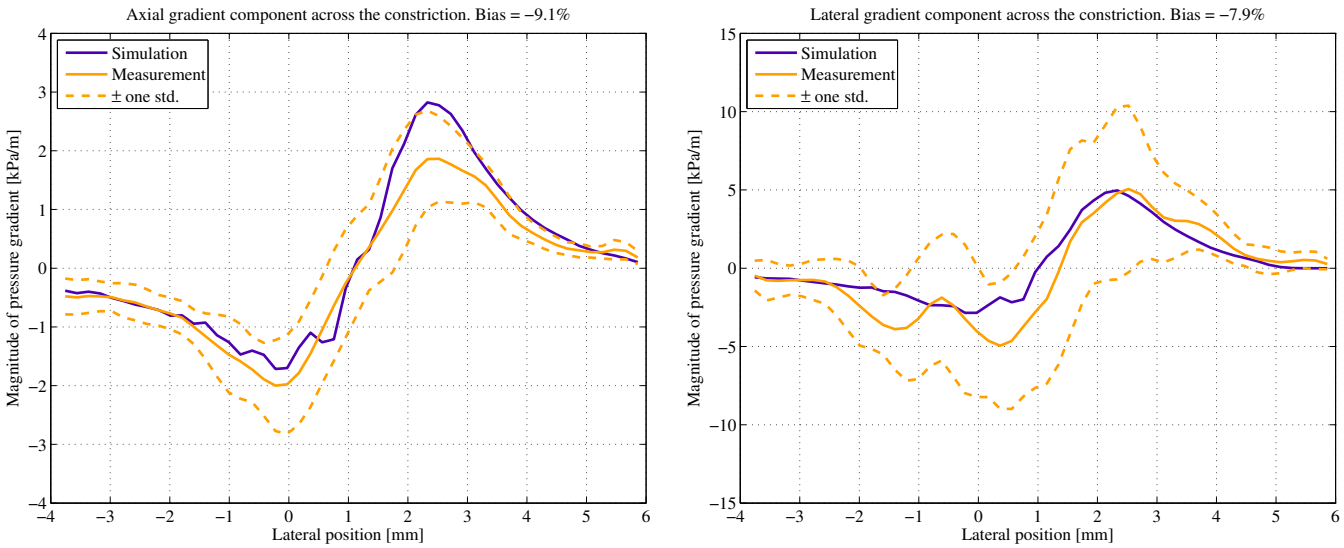

Figure 3. Estimated and simulated pressure gradients along the longitudinal direction of the constriction. The two graphs show the axial and lateral component of the pressure gradient, respectively.

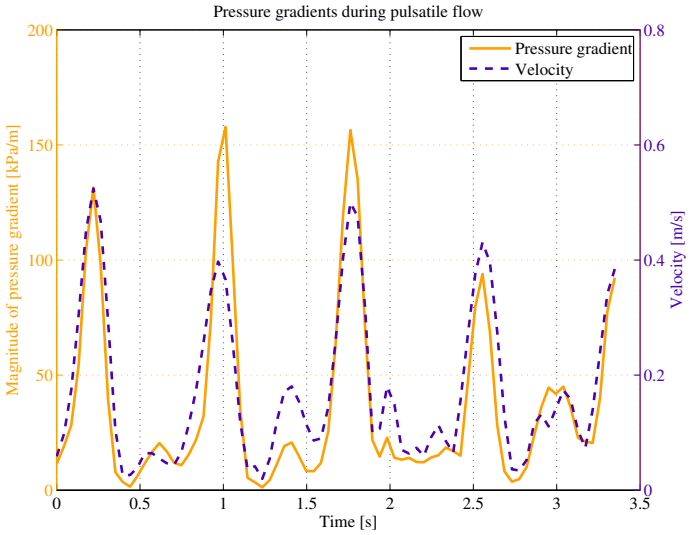

Figure 4. Estimated pressure gradients in pulsating flow together with the velocity of the fluid.

C. *In-vivo measurement*

An *in-vivo* study was performed by a medical doctor on a healthy volunteer. The study was made on the common carotid artery (CCA) using the linear array transducer at a pulse repetition frequency of 5.1 kHz, displaying 23 frames per second. Fig. 6 shows the estimated velocity fields and the pressure gradients during end-diastole and peak systole, respectively. The size of the estimated gradients are in some areas forty-times greater during peak systole than in end-diastole. This significant increase of the pressure gradients during peak systole is in agreement with the results obtained from the pulsating flow phantom. Thus, confirming that the size of a pressure gradient is highly governed by temporal velocity changes. This is especially the case in the CCA as the tortuous of the vessel is small, hence, the spatial velocity becomes unimportant. However, measuring pressure gradients in the carotid bulb or at its bifurcation would increase the role of the spatial acceleration as the flow patterns in these regions are more disrupted by the geometry of the vessel.

V. Conclusions

A non-invasive method for deriving pressure gradients using vector velocity ultrasound data has been presented. The pressure gradients were derived using the Navier-Stokes equation for incompressible fluids. The vector velocities inserted into the equation were estimated using the TO method yielding the two in-plane velocity components. The obtained pressure gradients were evaluated by comparison to a finite element simulation model, for which the geometry was obtained from MRI data. The employed method produced pressure gradients within a constricted flow phantom with magnitudes varying from -3 kPa/m to 10 kPa/m and from 5 kPa/m to 150 kPa/m for constant and pulsatile flow, respectively. An *in-vivo* study on the common carotid artery showed pressure gradients from roughly 20 kPa/m in end-diastole to more than 400 kPa/m in peak systole, indicating the dominant role of temporal velocity changes when estimating pressure gradients in the CCA. The advantage of using ultrasound for estimating pressure gradients is its capability of producing *in-vivo* images at a high frame-rate. This is crucial when measuring on a pulsatile flow environment.

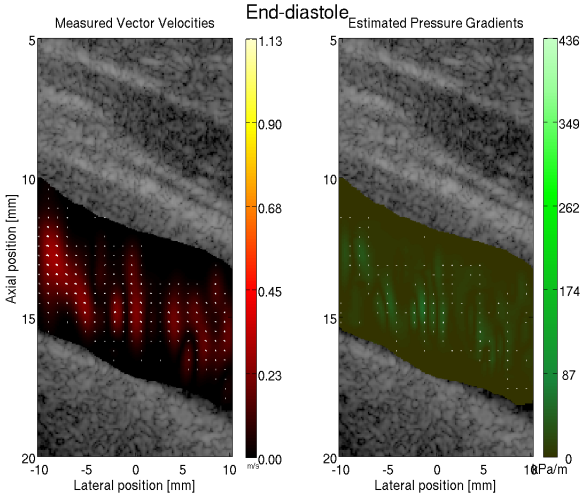

Figure 5. Vector velocity flow and pressure gradients measured on a common carotid artery in end-diastole.

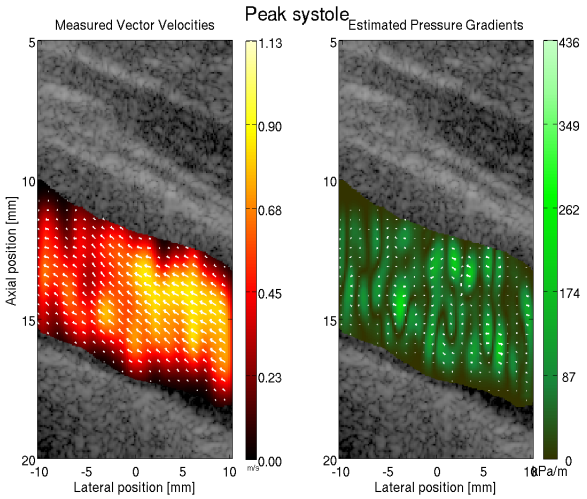

Figure 6. Vector velocity flow and pressure gradients measured on a common carotid artery in peak systole.

References

[1] D. S. Baim and W. Grossman, *Grossman's cardiac catheterization, angiography, and intervention*. Lippincott Williams & Wilkins, 2000.

[2] W. M. Fairbank and M. O. Scully, "A new noninvasive technique for cardiac pressure measurements: resonant scattering of ultrasound from bubbles," *IEEE Trans. Biomed. Eng.*, vol. 24, pp. 107–110, 1977.

[3] J. A. Jensen and P. Munk, "A New Method for Estimation of Velocity Vectors," *IEEE Trans. Ultrason., Ferroelec., Freq. Contr.*, vol. 45, pp. 837–851, 1998.

[4] M. E. Anderson, "Multi-dimensional velocity estimation with ultrasound using spatial quadrature," *IEEE Trans. Ultrason., Ferroelec., Freq. Contr.*, vol. 45, pp. 852–861, 1998.

[5] L. Prandtl, *Essentials of Fluid Dynamics*. London: Blackie & Son, 1952.

[6] N. B. Wood, "Aspects of fluid dynamics applied to the large arteries," *J. Theor. Biol.*, vol. 199, no. 953, pp. 137–161, April 1999.

[7] G. D. Smith, *Numerical Solution of Partial Differential Equations: Finite Difference Methods*. Oxford University Press, 1985.